Proceedings of the IPG 2023
International Pipeline Geotechnical Conference
IPG2023
23-24 November 2023, Bogotá, D.C., COLOMBIA

IPG2023-####

NUMERICAL MODEL, SOIL VS. BURIED PIPELINE INTERACTION IN ECUADOR

René Tipán[1], Carlos Mendoza[2], Pablo Caiza[3]

[1]Oleoducto de Crudos Pesados, Quito, Ecuador
[2]Universidad Central del Ecuador, Quito, Ecuador
[3]Universidad de las Fuerzas Armadas ESPE, Sangolquí, Ecuador

ABSTRACT

Ecuador has important oil pipelines whose continuous operation must be ensured by detailed studies of their behaviors. However, the difficult topography they cross, together with the climate, makes them especially vulnerable to landslides. This article develops a numerical model using finite elements that represent the pipeline immersed in the ground and subjected to displacements generated by permanent deformations of the ground. The geometry and loads of the model represent the effect of a slip predominantly transverse to the axis of the pipe. Specifically, the soil is characterized by a nonlinear Mohr-Coulomb model with parameters verified by geotechnical and soil mechanics tests. The soil-steel interface considers normal and shear stresses. The model is validated by applying it to a typical case located in the eastern foothills of the Andes in Ecuador. The model shows the behavior of a localized failure with a short-wave fold due to a phenomenon of longitudinal buckling in the pipeline. Furthermore, it is shown that the critical case is that of transverse loads plus an axial component.

Keywords: Pipeline; Landslide; Permanent ground deformation; Punctual estimation; Probability of failure.

NOMENCLATURE

Place nomenclature section, if needed, here. Nomenclature should be given in a column, like this:

α	alpha
β	beta

1. INTRODUCTION

This research work is motivated to develop a methodology to assess the degree of vulnerability of buried steel pipes intended for the transport of hydrocarbons before the occurrence of mass removal phenomena. This can be considered as an issue of particular importance for the country's geotechnics, given that the different oil pipelines that are guaranteeing the development of the national economy extend through the mountainous relief. Worldwide mass removal phenomena constitute 3% of the causes for oil spills, however, it has been seen that the frequency of landslides increases in the case of the Andes Mountain range up to 140 times more compared to the average value of the entire American continent [1]. For this reason, this research work presents the elaboration of curves that relate the degree of vulnerability to displacements generated by landslides and the flexural ductility limits of the pipe's constituent material, considering intrinsic characteristics of the pipeline such as diameter, wall thickness, manufacturing steel grade, among others, and extrinsic characteristics such as slide widths, geomechanically parameters, ground movement rates, etc.

2. MATERIALS AND METHODS

2.1 Geotechnical characterization

To calculate the stresses, strains and the actual interaction between the soil and the pipe, it was necessary to collect the following information:

- General description of the phenomenon that causes the permanent deformation of the soil.
- Classification and stratification of the soil.
- Soil cutting parameters.
- Dynamic parameters (Vp, Vs, Gs, Es, μs).
- Elastoplastic parameters (E, μ).
- Variation of groundwater levels.
- Evolution of displacements measured with instrumentation.

This information was obtained through the execution of a geotechnical reconnaissance plan, which consisted of in-situ mechanical tests, indirect tests (geophysical methods), and laboratory tests.

2.2 Displacement field associated with a polynomial.

For a better understanding of the acting phenomenon, it is necessary to outline the problem, that is, the interaction between the landslide and the pipeline. The buried pipeline is near the base of the landslide, which exhibits a preferential direction of lateral movement, undergoing permanent ground deformation (PGD) [2]. Figure 1 provides a clearer visualization of this scenario.

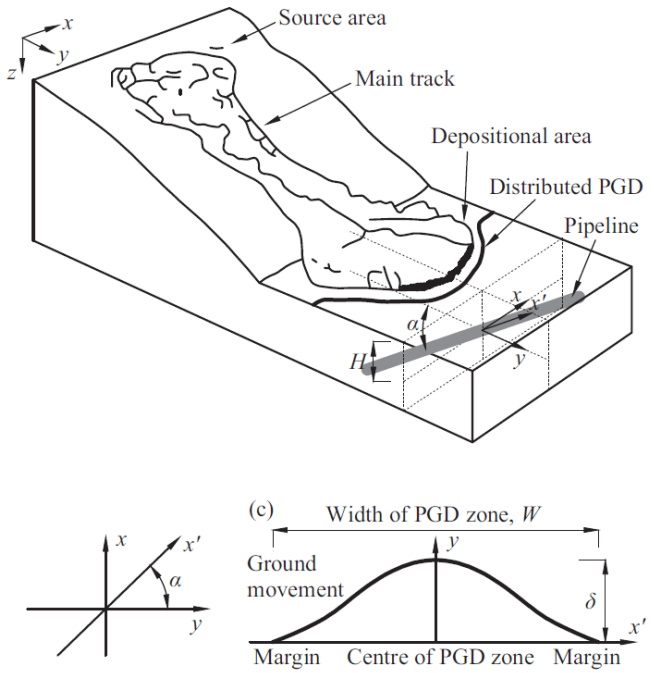

Figure 1: Illustration of the interaction issue between a landslide and the pipeline. Adapted from [2]

It's noticeable that the pipeline will undergo bending deformation due to the prescribed lateral displacement profile. Various research studies have put forth different empirical functions to describe the permanent ground deformation (PGD) as a boundary condition. Suzuki et al. (1988) and Kobayashi et al. (1989) [3, 4] employed a power-elevated cosine function with exponent 'n':

$$y(x) = \delta\left(\cos\frac{\pi x}{W}\right)^n \qquad (1)$$

x = represents the distance measured from the center of the permanent deformation zone.
δ = stands for the maximum lateral displacement of the soil, which decreases as x increases.
W = denotes the width of the permanent deformation zone.
The parameter 'n' should always be positive. A lower 'n' value will result in a wider distribution of ground discontinuity, while a higher 'n' value will create a more localized displacement profile.

2.3 Dealing with Uncertainties

Because soil shear parameters exhibit significant variation due to their high heterogeneity over short distances, precisely quantifying them becomes a complex challenge. To address this issue, the Rosenblueth point estimation method is employed. This method simultaneously considers the uncertainty and correlation of soil parameters. For this purpose, cohesion (C), friction angle (ϕ), and Young's modulus (E) are treated as significant random variables, modeled with a normal and symmetrical probability distribution.
The Rosenblueth point estimation method employs the mean, variance, and skewness coefficient as inputs, which are the first three statistical moments of a random variable. It's a simple yet highly accurate and powerful tool for evaluating statistical properties of a model involving various input random variables, whether they are symmetric or asymmetric, and whether they are correlated or not. Figure 2 illustrates how this method substitutes the continuous probability density function of the input random variable with two discrete mass points located on both sides of the mean. Estimation of statistical moments of the model's output is achieved by multiplying model outputs at these two mass points with weighted factors.

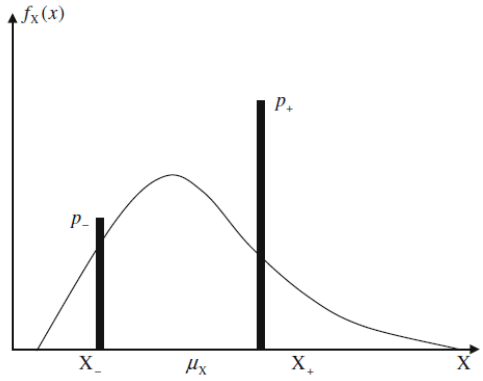

Figure 2: The Rosenblueth point estimation method. Adapted from [5]

2.3 Probability of failure estimation

Considering the mean (μξ) and standard deviation (σξ) of the duct deformation ξ, calculated using the Rosenblueth point estimation method, and if ξ follows a normal distribution, the likelihood of the deformation induced by the loads generated due to permanent ground deformation exceeding the yield deformation (ξy) of the pipeline steel can be estimated as:

$$Pof = 1 - \Phi\left(\frac{E[\xi]}{\sqrt{var[\xi]}}\right) \qquad (2)$$

Where:
Φ = represents the cumulative normal distribution function.

E[ξ] = denotes the expected value of the deformation, which is also known as its mean value.
var[ξ] = signifies the variance of the deformation, which under the square root becomes the standard deviation.
It's worth mentioning that, to estimate the probability of failure of the pipeline due to permanent ground deformation, the yield deformation of the pipeline material will be used as a threshold. This value is 0.5% for an API 5L-X70 steel with a yield stress of 525MPa.

2.4 Numerical model

The developed model considers soil parameters, considering a priori uncertainty for each of the random variables, as explained earlier. On the other hand, it incorporates the structure or pipeline with its well-known or predetermined properties. Since the aim of this research is to create a vulnerability curve for the pipeline when facing permanent ground displacements, while considering their interaction, it was appropriate to use a broad model. This means not considering the vertical or horizontal geometry of the pipeline, nor the terrain's topography. This approach allows the results obtained to be applied to other locations where soil properties fall within the adopted range of uncertainty. To numerically explore the effect of stresses caused by soil displacement on the pipeline, the general-purpose finite element software ABAQUS was used. This software considers the nonlinear behavior of both the soil and the pipeline, depicting significant deformations within the soil-pipeline system and the inelastic behavior of both materials.
Surrounding soil is modeled as a prism, 10 meters in width, 7 meters in height, and extending for a length of 130 meters. It is divided into three sections: a short 25-meter section, an intermediate 25-meter section, and a long 80-meter section. These divisions were made to investigate the distance at which the stresses generated in the pipeline due to permanent ground deformation dissipate, as well as to define the boundaries of the moving zone, as shown in Figure 3. An elevation of 7 meters is chosen to correspond to the soft soil layer depth determined by geotechnical studies.

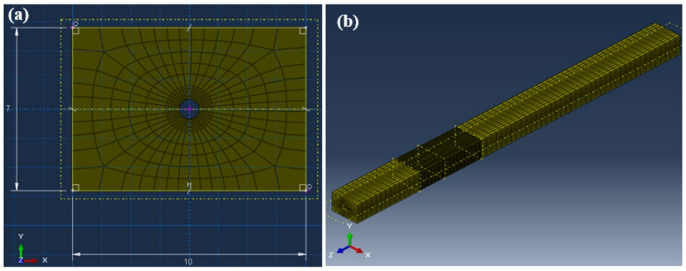

Figure 3: (a) Frontal view of the soil model. (b) Isometric view of the soil model, displaying a finer mesh in the area representing instability.

Elements of the C3D8R type with 8 nodes and reduced integration, referred to as "brick" elements, are chosen to model the surrounding soil. A notably finer mesh will be applied in the intermediate area, where instability is expected, to achieve a better understanding of the effects caused by the soil's forces on the pipeline.
The pipe is represented as a large-diameter, thin-walled cylinder without vertical or horizontal curves. Similarly, to the soil, it's divided into three sections: a short 25-meter portion, an intermediate 25-meter section, and a lengthy 80-meter stretch, to achieve better coherence between the soil mesh and the duct. The pipeline is embedded in the prism that simulates the soil, positioned at a 3.5-meter height measured from the center of the pipe to the top of the prism representing the surface. Four-node shell elements with reduced integration were employed to create the mesh for the pipeline segment. It has a diameter of 34 inches (863.6 mm), a wall thickness of 0.34 inches (8.74 mm), and a length of 130 meters. The pipeline is made of API 5L-X70 steel with a density of 7580 kg/m³, a Young's modulus E = 210 GPa, yield stress σ1 = 525 MPa, ultimate tensile stress σ2 = 640 MPa, and a Poisson's ratio ν = 0.292. Similarly, to the soil, the section presumed to be unstable has a finer mesh to enhance result detail. A plastic model of large deformations with isotropic hardening is used to describe the mechanical behavior of the pipeline.

2.5 Boundary conditions

As the soil undergoes displacement, both transverse and axial movements occur within the pipeline. The resistance generated by their interaction increases proportionally with the intensity of soil motion and its intrinsic properties. Considering this, it becomes necessary to establish boundary conditions that replicate the friction between the soil and the pipeline. This arrangement enables the pipeline to glide through the soil, consequently yielding the mobilized shear stress—an outcome directly governed by the friction coefficient μ. The corrosion protection coating (FBE) carries a value of μ = 0.6.
The edges of the prism representing the soil also have boundary conditions depicted in Figure 4. The bottom face will be restricted from displacement in the "Y" direction, as per the adopted coordinate system. The start and end edges will have displacement restrictions in the "Z" direction. The lateral edges, where the mesh appears denser, will be fixed in the "X" direction. In the central zone where the displacements caused by soil movement develop, there will be no lateral restrictions. The pipeline at its starting and ending points will have restrictions on displacement along the X, Y, and Z axes; however, it can rotate freely. According to Vazouras et al. (2010) [3], these ends can be conceptualized as springs that represent the flexibility provided by the pipeline's continuity. This results in a reduction in narrowing of the cross-sectional area due to tension-induced deformations. Nevertheless, as the same author demonstrates, a conservative approach to the phenomenon is to keep the ends fixed.
The deformation imposed on the soil due to slippage will adhere to Equation (1), applied in the section where the mesh is denser (Figure 4), as this region simulates the width of the slippage. At its center, the highest displacement value "δ" will be situated, with the ends—signifying the transition areas between stable and

unstable soil—exhibiting their minimum values. Additionally, a controlled scheme is employed wherein the demands progressively increase.

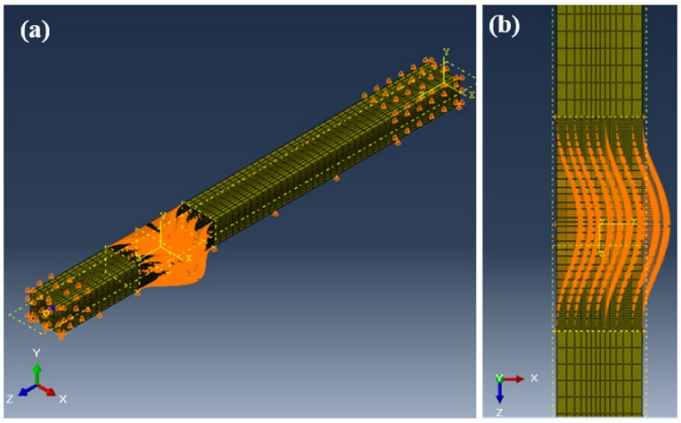

Figure 4: (a) Boundary conditions on the edges representing the soil. (b) Deformation in the soil caused by sliding.

2.6 Probabilistic modeling

Employing the Rosenblueth's point estimation method for k variables and factoring in significant soil random variables, namely cohesion (C), friction angle (ϕ), and elastic modulus (E), a probabilistic model was formulated to address the variability conditions described in Table A. The letter "P" symbolizes the weighted factor of each input random variable, the "+" sign indicates the interest random variable added to one standard deviation, and the "-" sign signifies the reciprocal condition, i.e., the interest random variable subtracted by one standard deviation.

Table A: Soil Variability for Rosenblueth's Point Estimation Probabilistic Model

Condition	Description
P_{+++}	For each random variable (C, ϕ, E), one standard deviation is added (μ+σ), meaning this soil can be interpreted as more cohesive, more frictional, and more elastic than its mean values.
P_{++-}	This soil can be interpreted as more cohesive and more frictional than its mean values, yet it's less elastic than its mean value, as one standard deviation has been subtracted (μ-σ).
P_{+--}	This soil condition indicates that it's more cohesive than its mean value, but one standard deviation has been subtracted from both the mean values of friction angle and elastic modulus.
P_{---}	In this soil condition, one standard deviation has been subtracted from each random variable's mean values, making this soil less cohesive, less frictional, and less elastic.
P_{--+}	This soil condition explains that both cohesion and friction angle have been reduced by one standard deviation, but their elasticity has been increased by the same proportion, meaning it's a more elastic soil.
P_{-++}	This condition states that the soil is less cohesive, more frictional, and more elastic than its respective mean values.
P_{-+-}	This soil condition denotes that it's less cohesive, more frictional, and less elastic than its mean values.
P_{-+-}	This condition shows that the soil is more cohesive, less frictional, and more elastic than its mean values.

2.7 Thresholds

The threshold is defined by the yield strain of API 5L-X70 steel, which has a value of ξ1 = 0.5%. In this manner, if the calculated strain values within the numerical model for various ground displacements are close to this value, the material will be at the limit of the elastic range. When this threshold is exceeded, it is considered failure, as the material will be in the plastic zone, resulting in permanent deformations. It's worth noting that the formation of a short-wave fold (wrinkle) due to local buckling in the compression zone or loss of containment in the tension zone will not be termed as failure.

The induced range of permanent ground displacements fluctuates between 0.2 and 2.0 meters. This means that for each displacement "δ," both strain and stress curves have been derived in relation to the model's length, accounting for each variability condition of soil properties at the study site.

2.8 Input data model

Table B displays the obtained input parameters used for calibrating the numerical model. Since the soil is a heterogeneous medium with significant spatial variability in its mechanical and shear properties, the presented values correspond to the mean of a normal distribution for each variable (cohesion, friction, and elastic modulus).

Table B: Input parameters for finite element model calibration

Item	Description	Symbol	Value	Unit
Pipeline	Material	-	API 5L-X70	-
	Outer Diameter	D	863.60	mm
	Wall Thickness	t	8.74	mm
	Density		7580.00	kg/m3
	Young's Modulus	E1	210000.00	MPa
	Yield Stress	σ1	525.00	MPa
	Yield Strain	ξ1	0.50	%
	Ultimate Tensile Stress	σ2	640.00	MPa

	Strain at Failure	ξ2	3.50	%
	Poisson's Ratio	ν	0.29	
Soil	Unit Weight	γ	14.00	KN/m3
	Friction Angle	φ	4.00	°
	Cohesion (Undrained Shear Strength)	Cu	0.028	MPa
	Young's Modulus	E	17.50	MPa
	Poisson's Ratio	ν	0.37	
Interface	Coefficient of Friction	μ	0.60	
Coating	Depth of Buried Pipe	H	3.50	m
PGD	Range of Permanent Ground Deformation	δ	0.1 - 2.0	m
	Width of Unstable Zone	W	25.00	m

Using Rosenblueth's point estimation method, for the multivariate model and under the soil variability conditions conceptualized in Table A, cohesion, friction, and elastic modulus values are derived (Table C). These values are then used to generate multiple runs of the numerical model, each corresponding to a distinct scenario.

Table C: Variability values for soil geotechnic parameters

CONDITION	C (Pa)			ϕ (°)			E (Pa)		
	-σ	μ	+σ	-σ	μ	+σ	-σ	μ	+σ
	-	**28E3**	-	-	**4**	-	-	**17E5**	-
P+++	-	-	42E3	-	-	10	-	-	25E6
P++-	-	-	42E3	-	-	10	1E7	-	-
P+--	-	-	42E3	0	-	-	1E7	-	-
P---	21E3	-	-	0	-	-	1E7	-	-
P--+	21E3	-	-	0	-	-	-	-	25E6
P-++	21E3	-	-	-	-	10	-	-	25E6
P-+-	21E3	-	-	-	-	10	1E7	-	-
P+-+	-	-	42E3	0	-	-	-	-	25E6

2.9 Failure modes

In accordance with Vazouras et al. (2015) [4], the performance assessment of buried pipelines subjected to ground-induced loads may encompass, but is not restricted to, the following failure criteria:

Maximum Tensile Strength

Tensile stresses can induce fracture in the pipeline wall at zones with material defects, welds, or areas of high stress concentration. This is regarded as an ultimate strength limit condition associated with the loss of containment in the pipeline. Vazouras et al. (2015) consider a 3% longitudinal deformation as an appropriate indicator for evaluating this limit state. Moreover, this criterion is adopted in two international codes: the European Committee for Standardization EN 1998-4, Provisions for seismic actions on buried steel pipelines, and the American Society of Civil Engineers ASCE MOP 119, Provisions for seismic action on buried steel water pipelines.

Local Buckling

Compressive stresses can lead to local buckling in the pipeline, resulting in the formation of a short-wave fold or wrinkle. This type of failure also represents a limit state of the pipeline's strength. Usually, a wrinkle develop does not necessarily imply loss of containment. However, excessive deformation of the fold in the buckled area, along with excessive tension on the side opposite to the buckling, can lead to fractures in the pipeline wall.

Cross-Sectional Distortion

Longitudinal bending causes a phenomenon of crushing or ovalization of the pipeline's cross-sectional area, which can render the pipeline unusable within operational parameters. The distortion factor "f" is a dimensionless parameter expressed as $f = \Delta D/D$, where ΔD represents the maximum change in diameter. A limit state may occur when the cross-sectional distortion reaches 15% relative to the original section, that is, $f = 0.15$

3. RESULTS AND DISCUSSION

The interpretation of the results obtained from numerical modeling will be conducted considering four key aspects: deformation, stresses, stress-strain relationship, and structural fragility or vulnerability as such.
Regarding the results presentation, two indicative lines, termed as generators, were introduced onto the structure. Line "A," as depicted in Figure 5, lies within the region directly influenced by the sliding force, referred to as the "compression zone." On the other hand, line "B" is positioned in an area not directly subjected to soil thrust but deforms as the soil displacement grows, constituting the "tension zone."

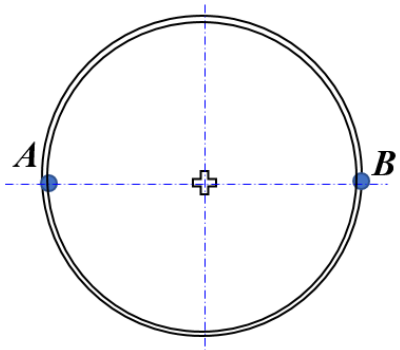

Figure 5: Generators. Line "A" - compression zone. Line "B" - tension zone.

3.1 Deformations

Figure 6 illustrates the pipe's deformation according to the imposed soil displacement pattern (δ) (Equation 1) within the range of 0.0 to 2.0m. For δ values between 0.0 and 1.1m, there are no discernible distortions in the geometry. Nevertheless, as δ increases, the pipe section undergoes buckling, both in the central area of the unstable region and at the transition zones or sliding boundaries.

Sheng et al. (2017) [5, 6] concluded in their study that the maximum stress and deformation values gradually increase as the sliding movement intensifies, and furthermore, their limiting values appear in the areas that seem to represent a joint between the sliding and non-sliding regions. This investigation fully aligns with the conclusion. However, the primary distinction lies in the equation representing displacement. Sheng employs a uniformly distributed displacement across the central zone, whereas in the present analysis, the displacement pattern follows a sinusoidal shape, allowing us to observe the gradual development of deformations and stresses until reaching a δ_{max} in the central area.

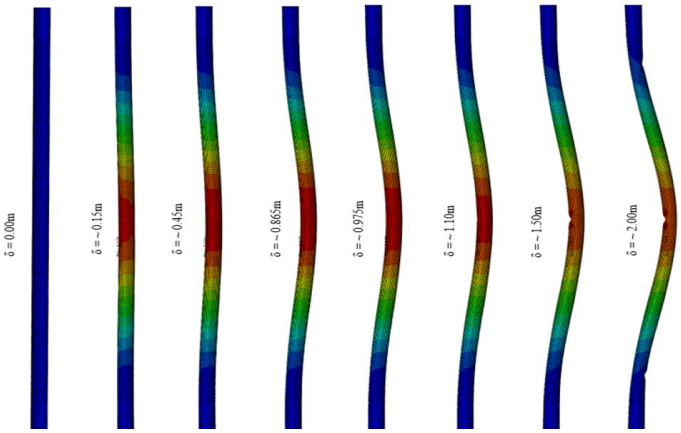

Figure 6: Permanent ground deformation over the pipeline, ranging from 0.0 to 2.0m.

API 5L X70 steel has a yield strain (ξ_1) of 0.5%, meaning that deformations are considered plastic beyond this threshold. Figure 7 demonstrates that in transition zones, δ > 0.40m is necessary to surpass the yield limit. However, in the central zone, where the displacement is at its maximum, δ > 1.00m exceeds this value (ξ_1). In the tension zone (Figure 35), the phenomenon is reversed. In the central part, the displacement that exceeds ξ_1 is greater than 0.4m, while in the transition zones, a δ ≥ 2.0m is required. Vazouras, Karamanos, and Dakoulas (2010) [3] studied a similar phenomenon where the pipe is influenced by the displacement from a fault perpendicular to its axis. The fault's width is only 0.33m. Based on this, a parallel can be drawn to the transition zones in this study, where the distinction between sliding and non-sliding regions is also evident.

Vazouras' study additionally indicates that with displacement values greater than 0.67m in the compression zone, the pipe initiates the phenomenon of local buckling, causing distortion of its wall. The values obtained in the current analysis closely approximate those stated by Vazouras. However, the slight variation may be attributed to the selection of soil shear strength parameters. The surrounding soil considered in this study is classified as soft clay, with Young's moduli following a normal distribution with an average of 17.5MPa and a range between 10MPa and 25MPa, while Vazouras considers two types of clays, soft clay with E = 25MPa, and firm clay with E = 100MPa.

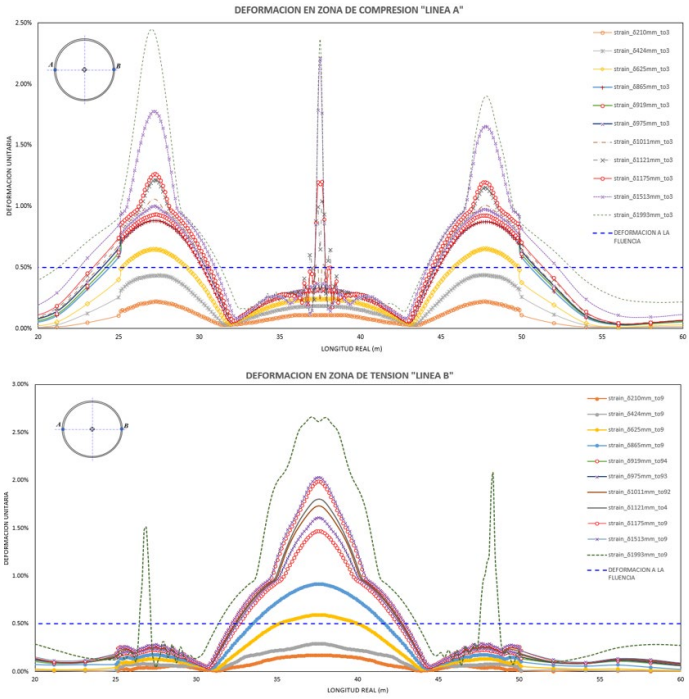

Figure 7: Strain vs. Length, in the compression and tension zones, for the range of permanent ground deformations between 0.0 and 2.0m.

It is important to note that, in accordance with the measurements taken in the field, the OCP pipeline experienced failure with a displacement of 0.345m in the central zone of the landslide. As mentioned earlier, a δ>1.0m is required to initiate the failure process. However, this scenario corresponds to soil with P+++ variability (Table A, C), indicating that it is stiffer and exhibits better shear resistance than the soil measured in the field.

Figure 8 illustrates how steel deformation changes with (δ) based on different ground variability conditions. The parameters related to soil shear strength (C and ϕ), as well as its Young's modulus, are also adjusted following a normal distribution. These parameters apply to soft soil. The graph shows that the envelope is bounded by curves representing P++- and P--+, indicating that less rigid soil requires a larger displacement (δ) to reach the steel's yield strain compared to stiffer soil. However, when shear strength parameters (C and ϕ) are reduced (P---), the curve shifts left, while an increase (P+++) causes the curve to move in the opposite direction. This demonstrates that regardless of whether the soil allows extensive deformation or not, its shear

strength characteristics significantly impact the pipeline's structural behavior.

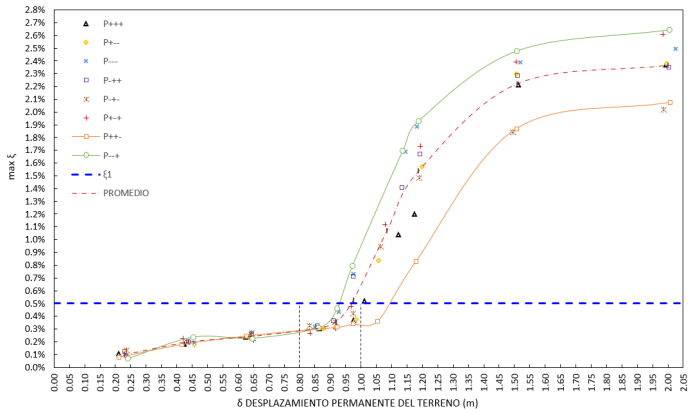

Figure 8: Deformation vs. permanent ground deformation. Landslide central zone in the numerical model.

3.2 Stress Behavior

In the initial stage of local buckling (Figure 9a, 9b), slight ripples on the pipeline surface are observed, indicating the concentration of compressive stresses. As the displacement increases, one of these ripples becomes dominant and rapidly transitions from compression to tension (Figure 9c, 9d), leading to distortion in the pipeline wall. Vazouras (2010) refers to the same behavior and notes its correspondence with experimental observations carried out by other researchers. However, it is crucial to emphasize that this phenomenon occurs not only at the point of maximum displacement but also in areas simulating the transition between stable and unstable soil.

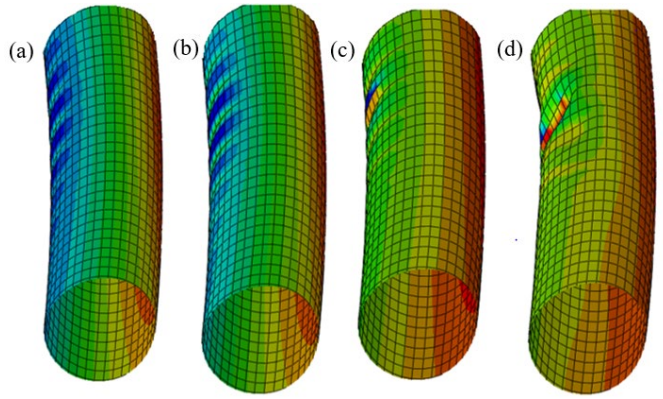

Figure 9: Stages of stress variation and wall distortion in pipeline

Figure 10 illustrates stress plotted against the length of the unstable area for various (δ) values within the compression zone (line A). The graph reveals that stresses in the central portion reach the yield stress σ_1 when δ>0.80m, and in the transitional zones, tension stresses of equivalent magnitude arise at the same (δ) levels. As the loading intensifies (δ), tension stresses emerge within the compression zone, spanning a length of 5m in the central region. These stresses exhibit the unfolding of the local buckling phenomenon, progressing from the gradual development of mild undulations to the sudden formation of a wrinkle that distorts the pipeline wall. This distortion concentrates tension stresses to the extent of even reaching the ultimate stress σ_2.

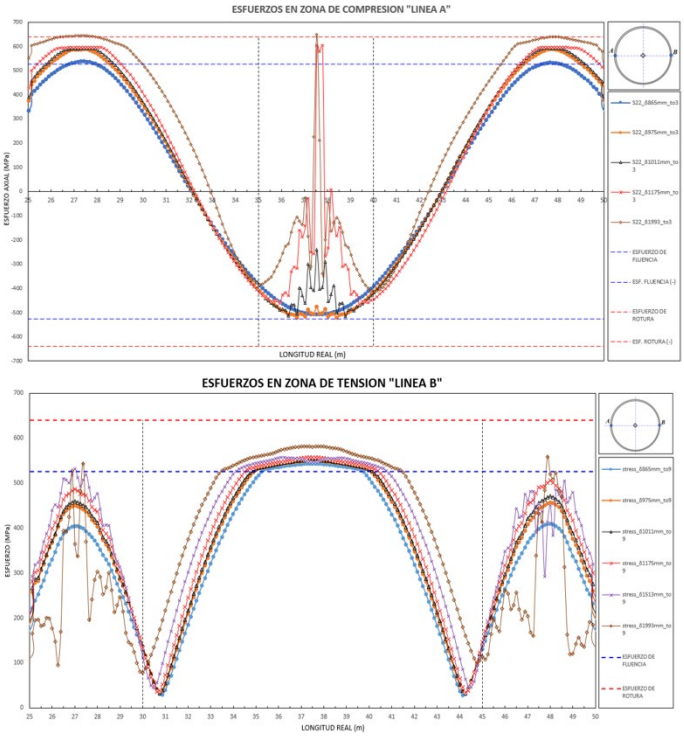

Figure 10: Stress vs. Length relationship, both the compression and tension zones, between 0.8 and 2.0m permanent ground deformation.

In the tension zone (line B), a similar phenomenon occurs in the central area. However, within the transitional zones, compressive stresses emerge. As the displacement (δ) increases, these stresses lead to the distortion of the pipeline wall due to local buckling. The key distinction lies in the fact that δ must surpass 1.20m to initiate this specific distortion. Conducting analyses for all proposed soil variability conditions, Figure 11 demonstrates that when δ<0.80m, the pipeline remains within the elastic range. This outcome closely aligns with the observations of Sheng et al. (2017), who report stress levels ranging from 240 to 566 MPa within the displacement range of 0.10 to 0.80m. Despite this concurrence, it is essential to emphasize that due to the steel's properties considered in their analysis, these stress levels approach the yield stress. It is noteworthy that in this study, the pipeline's steel does not reach this limit.

Under the same soil variability conditions, P--+ and P++-, examined in the deformation scenario, it is observed that as the soil's stiffness increases, the stress in the pipeline at δ=0.98m is 589 MPa. Conversely, when soil stiffness decreases, the stress reduces to 526 MPa. This demonstrates that stiffer soil, having

lesser deformation capacity, exerts greater restraint on the pipeline, causing stresses to be absorbed in a more pronounced manner by it.

Therefore, based on the above, it can be concluded that a displacement (δ) of 0.80m in the central area of the landslide is suitable as a threshold, as both the deformations and stresses exceed the elastic range beyond this point. However, it's essential to consider that, in the transitional zones, the limit of yield deformation is reached with displacements greater than 0.4m. Furthermore, to surpass the stress limit, δ>1.20m is necessary. Hence, these transitional zones, being subjected to a boundary condition between stable and unstable ground, behave like fixed supports, causing deformations to concentrate.

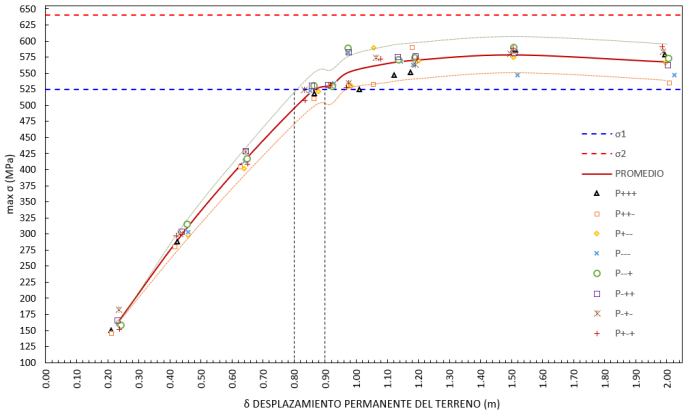

Figure 11: Stress as a function of permanent ground deformation

3.3 Stress – strain analysis

To validate the numerical model's results, Figure 12 compares the stress-strain curve, which represents the average of all soil variability conditions at the point of maximum displacement, with the tension test curve obtained from a laboratory experiment performed on a pipe sample. The test curve reveals that the steel's elastic range reaches its limit at a stress (σ) of 455 MPa, whereas in the numerical model, this occurs at σ=520 MPa. This discrepancy can be understood by considering the site conditions as a criterion. The laboratory test necessitates extracting a sample from the pipe, yielding results that are representative of that sample. In contrast, the numerical model is calibrated for the entire geometry, thereby incorporating the flexibility contributed by the entire assembly. As a result, the steel in the numerical model reaches its elastic limit at a higher stress level compared to the laboratory test. The phenomenon is reversed in the yield zone: when the strain (ξ) reaches the yield limit (0.5%), the tested sample exhibits a stress of σ=579 MPa as its maximum, while the numerical model demonstrates a lower stress level of σ=551 MPa. As explained above, this difference arises due to the interaction between the pipe and the soil, which is significantly influenced by their shear strength and stiffness parameters.

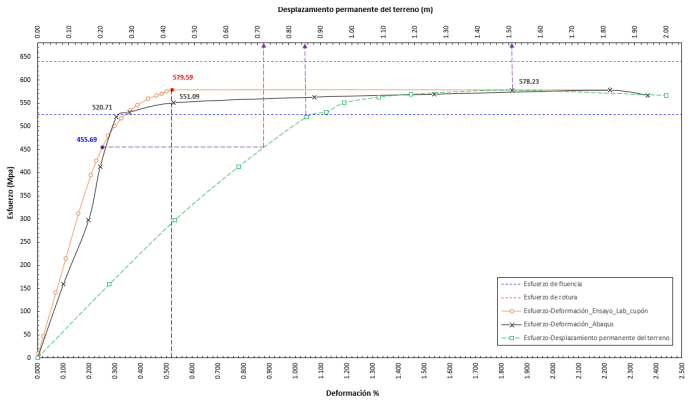

Figure 12: Stress-strain curve compared with the curve obtained from the laboratory tensile test on a sample taken from the API 5L-X70 steel pipe.

3.4 Structural fragility

The structural fragility [7] curve (Figure 13) depicts the probability of exceeding steel's yield strain concerning permanent ground displacement. For displacements smaller than 0.80m, the probability approaches zero. However, as loading increases, this probability escalates rapidly. Notably, within the range of 0.85m to 0.95m, just a 10cm interval, the probability of encountering plastic deformations is 16 times higher. If we position δ=0.95m on the stress-strain graph (Figure 12), a stress (σ) of 545 MPa and a strain (ξ) of 0.46% are obtained. Although the strain is nearly reaching the yield limit, the stress surpasses this limit by 20 MPa, which, in magnitude, seems insignificant at first glance. Subsequently, when the ground displaces by an additional 15cm, i.e., δ=1.10m, the probability of exceeding the yield strain reaches 98%. Again, from Figure 12, a stress of 565 MPa and a strain of 1.08% are obtained. Analyzing this behavior carefully, it's evident that a mere 20 MPa stress, caused by a 15cm displacement, is enough to double the steel's deformation limit.

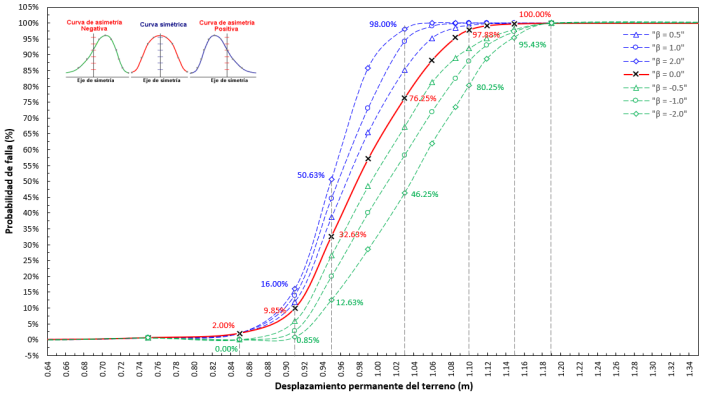

Figure 13: Structural fragility curve in relation to permanent ground deformation, for the following coefficients of asymmetry of soil random variables: Red line, symmetric β=0; Dashed blue lines, positive asymmetry (to the left) β>0; Dashed red lines, negative asymmetry (to the right) β<0.

Therefore, displacements that may appear insignificant at first glance can lead to stress and deformation levels that exceed acceptable limits.
One of the crucial considerations that describes the probability of failure in this study is the fact that the soil random variables (C, ϕ, and E) are fitted to a normal distribution with a skewness coefficient β=0, indicating that these data points are equally dispersed around the mean value. This assumption presents an ideal scenario. However, it's necessary to analyze what happens to the probability when the skewness of the variables deviates from zero. Having β>0 implies that there is a bias in the data, with greater dispersion to the left of the mean value. This can be interpreted as soils having lower shear strength and higher deformability. Conversely, when β<0, the data exhibits greater dispersion to the right of the mean value, indicating soils with better shear strength characteristics and higher stiffness.
Figure 13 depicts fragility curves considering the variation in β. It's observed that when the skewness is towards the left, the probability of failure increases for the same displacement value (δ). The inverse phenomenon occurs when the skewness is towards the right. This once again highlights the significant impact that the surrounding soil has on the structural behavior of the pipeline.

3.5 Discussion

The purpose of this research was to develop a model that considers the physical conditions and structural behavior characteristics of the OCP pipeline when subjected to lateral ground sliding forces. This was achieved using sophisticated finite element techniques that capture the nonlinearity of the problem. The goal was to reproduce the observed behavior in real-world scenarios and enable the extrapolation of results to even more extreme conditions.
The outcomes obtained in this project indicate that, following the application of numerical modeling using finite elements and considering the displacements associated with Equation 1, which describes the soil movement using a cosine function, as well as factoring in the variability of soil mechanical and shear properties (C, ϕ, and E) through a probabilistic analysis, the structural behavior of the pipeline is largely influenced by the properties of the surrounding terrain. It exhibits greater deformation in soils with lower stiffness and less shear strength compared to those with more favorable characteristics.

Similar model was developed by Thompson N. (2009) [8] for OCP, following a rupture caused by ground movement resulting from a geohazard. This study was specifically focused on replicating the exact conditions under which this scenario occurred. One of its key assumptions is that the equivalent displacement experienced by the pipeline corresponds to 95% of the soil movement. However, according to the present research, this assumption might not accurately reflect real conditions. As depicted in Figures 8, and 11, the stress and deformation caused by soil movement are closely dependent on the mechanical and shear strength soil properties. In other words, if soil is more rigid, it will restrain the pipeline from easily displacing, leading to greater restriction on the pipeline. This causes the pipeline to absorb a significant portion of force, resulting in stress and deformation accumulation. On the contrary, when the soil is soft, it allows the pipeline to move more easily, absorbing force to a lesser extent due to the surrounding soil mass exerting less restraint.
Thompson's assessment does not take into consideration the surrounding soil relevance. He validates this demonstrating that over 34% of buckling modes derived from his model predict the formation a wrinkle due to localized buckling resulting from a critical load. Furthermore, he specifies that such a load is achieved with a peak displacement of 0.81m, a value which aligns closely with threshold value (0.80m) determined in this research. Nevertheless, it is important to clarify that threshold adopted in this study simply marks a point beyond which elastic deformations become irreversible and does not signify a value below which the pipe wall experiences distortions. The underlying reason for this disparity lies once again in the pivotal role that soil characteristics play in the pipeline's structural behavior. Additionally, in Vazouras's (2010) publication titled "Finite Element Analysis of Steel Pipes under Geological Fault Displacements," the conclusion is drawn on properties of surrounding soil apply a substantial influence on the pipe's deformation process. Among Vazouras's results, is evident that under the same displacement induced by fault movement, bending stresses and deformations are more pronounced in firm clay compared with those observed in soft clay.
A relevant aspect that is common, both present research and the study conducted by Thompson, as also illustrated in Vazouras's publication, is the phenomenon of stress propagation in pipeline wall due to solicitations occurs gradually (Figure 9). This leads to concentration of compressive stresses in the flexed zone, resulting in formation of undulations until one of them becomes dominant and rapidly shifts its stress state from compression to tension. However, Thompson emphasizes that not only axial compressive load is sufficient, but it must necessarily be combined with a bending component and internal pressure, otherwise, the pipeline wall will tend to collapse rather than forming wrinkles. The operational pressure load is not considered in the model of this research because, in accordance with Vazouras (2010), the presence of internal pressure causes a slight decrease in the critical displacement. This is due to the adverse effect it has on the pipe wall's deformability. Nevertheless, it is acknowledged that more accurate results could be obtained by incorporating the operational pressure load, leaving this aspect open for future investigations.

Lastly, it's important to highlight that none of the mentioned studies consider the significant soil variables to understand how the pipeline's probability of failure responds to soil movement. While obtaining fragility curves is certainly valuable, it's important to note that conducting a probabilistic analysis requires having samples that encompass a meaningful amount of data for the problem at hand. As a result, the shortage of field data means that there are no practical empirical fragility curves

available that capture the interplay between soil and pipeline against which the ones obtained in this study can be compared. Globally, only a limited number of research endeavors have successfully generated such curves, addressing the issue through analyses involving numerical methods.

Ni et al. (2018) conducted a study in which they likened the pipeline to beam supported by Winkler-type springs that provide lateral and axial resistance. However, they omit the 3D effect, which encompasses the possibility of pipe settlement or uplift and of shear forces generation due to friction resulting from soil interaction. They did this to obtain a representative dataset (one million cases) that forms a suitable framework to cover the probability space dictated by soil uncertainties. This scenario combinations resulting in sufficiently large sample for conducting probabilistic analysis, while accounting for the 3D effect of problem, would not be computationally feasible. Therefore, considering all the mentioned factors, this study is deemed innovative as it captures soil variability parameters using the Rosenblueth point estimation method. This method doesn't use an extensive dataset for probabilistic analysis, as it employs the first three moments of each random variable and replaces their probability density function with two discrete mass points. This greatly synthesizes the scenario combination process.

Furthermore, this methodology offers the capability to sensitize the skewness coefficient β, yielding curves that portray the probability of failure when the geotechnical characteristics of the soil vary around a mean value. Once again, this underscores the fundamental role of these characteristics in the structural performance of the pipeline under the stresses induced by soil movement (Figure 13). One of the significant advantages of Fragility curves is that they constitute a pivotal tool for prevention, and they can be employed to mitigate vulnerability. This can be achieved without the necessity for a mass soil movement event to occur.

4. CONCLUSION

Examining topographic monitoring, the displacement measured in pipeline without surrounding soil is 36% greater than pipe was enclosed by it. However, a wrinkle was still not observed. This demonstrates that surrounding soil caused resistance effect to displacement, preventing the pipe from deforming freely and causing stress accumulation in structure until reaching failure.

Correlating the topographic monitoring data with pattern provided by Equation (1), numerical model demonstrates that pipeline structural behavior has a pronounced dependence on the geotechnical properties of the surrounding soil. Furthermore, it indicates that greater deformation occurs in pipeline when placed in soils with lower rigidity and limited shear strength compared to soils with more favorable attributes.

Displacement $\delta = 0.80$m in landslide central area is suitable threshold, as beyond this point, both deformations and stresses exceed the elastic range. However, it's essential to consider that, in transition zones, yielding deformation limit is reached with displacements greater than 0.4m. Additionally, to exceed the stress limit, displacements $\delta > 1.20$m, are necessary. Therefore, these zones, being subject to boundary condition between stable and unstable ground, behave like encastre fixations, causing concentrate stress.

Finally, in structural fragility curve we observed that displacements greater than 0.80m, pipe probability of failure grows rapidly in displacement intervals between 10 and 15 cm, therefore, from threshold, small movements are capable to generate stresses and deformations in pipeline steel that would lead to exceed yield limit and even to form short-wave folds in its wall due to local buckling.

ACKNOWLEDGEMENTS

Warm thanks to the OLEODUCTO DE CRUDOS PESADOS - ECUADOR, which proficiently provided the data and field studies that were essential for the development of this research, in addition to the licensing of specialized software.

REFERENCES

[1] González, M. (2010). Análisis de vulnerabilidad de tuberías sometidas a deslizamientos. Bogotá: Universidad Nacional de Colombia.

[2] Ni, P., Mangalathu, S., & Yi, Y. (2018). Fragility analysis of continuous pipelines subjected to transverse permanent ground deformation. Soils and Foundations, 58(6), 1400-1413.

[3] Vazouras, P., Karamanos, S. A., & Dakoulas, P. (2010). Finite element analysis of buried steel pipelines under strike-slip fault displacements. Soil Dynamics and Earthquake Engineering, 30(11), 1361-1376.

[4] Vazouras, P., Dakoulas, P., & Karamanos, S. A. (2015). Pipe–soil interaction and pipeline performance under strike–slip fault movements. Soil Dynamics and Earthquake Engineering, 72, 48-65.

[5] Zhang, L., Fang, M., Pang, X., Yan, X., & Cao, Y. (2018). Mechanical behavior of pipelines subjecting to horizontal landslides using a new finite element model with equivalent boundary springs. Thin-Walled Structures, 124, 501-513.

[6] Zhang, S. Z., Li, S. Y., Chen, S. N., Wu, Z. Z., Wang, R. J., & Duo, Y. Q. (2017). Stress analysis on large diameter buried gas pipelines under catastrophic landslides. Petroleum Science, 14, 579-585.

[7] Vázquez-Guillén, F., & Auvinet-Guichard, G. (2018). Fragilidad estructural de componentes ante incertidumbres no gaussianas correlacionadas. Ingeniería, investigación y tecnología, 19(1), 101-112.

[8] Thompson N. (2009) Part 2 Report – Findings and Expert Opinion on the Cause of Failure of OCP Pipeline at KM point 127.94. Información propiedad del Oleoducto de Crudos Pesados S.A

